JOURNAL OF AIRCRAFT
Vol. 39, No. 2, March–April 2002

Effect of Thrust on Bending–Torsion Flutter of Wings

Dewey H. Hodges,* Mayuresh J. Patil,† and Seungmook Chae‡
Georgia Institute of Technology, Atlanta, Georgia 30332-0150

The effect of thrust on the flutter of a high-aspect-ratio wing is investigated. The wing is represented by a beam using a nonlinear mixed finite element method. Aerodynamic forces are calculated using a finite state, two-dimensional unsteady aerodynamic model. The effect of thrust is modeled as a follower force of prescribed magnitude. Without the thrust force, the wing is shown to become unstable for freestream airspeeds greater than the flutter speed. On the other hand, in the absence of aerodynamic forces, the wing becomes unstable for values of the thrust in excess of a critical magnitude of the force. When both effects are present, the airspeed at which the instability occurs depends on the thrust magnitude. For validation, an analytical solution for the in vacuo case (accounting only for the effect of thrust) was developed and shown to match closely results from the numerical method. Parametric studies show that the predicted stability boundaries are very sensitive to the ratio of bending stiffness to torsional stiffness. Indeed, the effect of thrust can be either stabilizing or destabilizing, depending on the value of this parameter. An assessment whether or not the magnitude of thrust needed to influence the flutter speed is practical is made for one configuration.

Introduction

FLUTTER of flexible structures due to aerodynamic effects is an old and practical problem, and many papers and books have been written about various aspects of it (for example, see Refs. 1–3). It is also well known that follower forces can induce flutter. The well-known Beck problem,[4] a cantilever beam excited by an axially compressive follower force, is a commonly analyzed problem in the literature. Indeed, there are now quite a few papers and a few books devoted to the stability of flexible structures loaded by follower forces. For example, see Refs. 5–7 for cantilever beams and Refs. 8–10 regarding the stability of a free–free beam subjected to a follower force.

When it is considered that engine thrust can be represented as a follower force, it is possible that thrust could lead to instability of the wing. Even if the thrust force were not high enough to induce instability on its own, it is quite likely that thrust could interact with other destabilizing mechanisms, for example, aeroelastic flutter. Even for propeller-driven aircraft, thrust could be important although, in the case of proppeller-whirl flutter, the thrust follows the propeller tip-path plane rather than the nacelle. For stiff propellers, however, it would nearly follow the nacelle. The effect of thrust on the flutter speed may be important, especially in the case of aircraft with very flexible wings. If thrust were to lead to a lowering of the aeroelastic flutter speed, one would certainly want to know about that to make appropriate adjustments in the design. Even if thrust were to increase the flutter speed, this could lead to an overly conservative design. In either case, the inclusion of thrust effects in flutter analysis should lead to a more complete analysis.

In spite of the huge body of literature on the aeroelasticity of lifting surfaces, there is very limited literature concerning the effects of the thrust of a wing-mounted engine on aeroelastic flutter. Indeed, in contrast to the significant number of papers that deal with various aspects of Beck's problem[4] (cantilevered beam loaded by an axial follower force), the problem of a cantilevered beam excited by a transverse follower force has not received much attention in the literature. This type of system was first considered in a stability analysis by Como.[11] By assuming a rigid body with specified mass and moments of inertia attached to the tip and neglecting the distributed mass of the beam, he obtained an analytical value for critical load. Wohlhart[12] extended Como's work to include the distributed mass and allowed the position of the added mass, moments of inertia, and the follower force (all at the same point) to vary. This excellent paper presents an extensive parametric study, taking into account all relevant parameters.

Restricting the location of the force and rigid body to the free end, Feldt and Herrmann[13] investigated the flutter instability of a wing subjected to the transverse follower force in the presence of airflow. Therein it was reported that an increase in tip mass always stabilizes the system, but according to Wohlhart,[12] this is not always true if one considers only the thrust-induced flutter. Feldt and Herrmann[13] considered only one value of the ratio of bending stiffness to torsional stiffness in their study, a value for which thrust is destabilizing. Moreover, the thrust-induced flutter results presented in Ref. 13 do not agree with those in Ref. 12.

It is the objective of the present study to determine whether or not the thrust of wing-mounted engines might have any effect on the aeroelastic flutter of wings. To carry out this objective, we first develop the analytical solution for instability due to thrust alone, without consideration of aerodynamic effects. This solution is then used for validating the finite element methodology for determining the influence of thrust on the aeroelastic stability. A mixed finite element method is then used to compute the instability boundary of the system under the influence of both effects. A parametric study focusing on the influence of the ratio of bending to torsional stiffness is also conducted. Finally, the thrust required to maintain the trim condition of a complete airplane model is estimated at various speeds and is used to determine the range of thrust values that can be considered as realistic.

Analysis of Thrust-Induced Flutter

Consider a cantilevered beam with elastic axis along the x_1 direction and with cross-sectional coordinates x_2 and x_3 as shown in Fig. 1. The beam has torsional stiffness GJ and bending stiffnesses EI_2 and EI_3, with $EI_3 \gg EI_2$. Denote the displacements as u_i with $i = 1$, 2, and 3 along x_i directions, and denote the section rotation due to torsion as θ_1. For the purpose of analysis, we introduce two sets of dextral triads of unit vectors, one fixed in an inertial frame of reference, $\boldsymbol{a}_i$, with $i = 1$, 2, and 3, along x_i, and the other fixed in the cross-sectional frame of the deformed beam, $\boldsymbol{B}_i$ with $i = 1$, 2, and 3.

Received 12 June 2001; revision received 8 November 2001; accepted for publication 6 December 2001.

*Professor, School of Aerospace Engineering. Fellow AIAA.
†Postdoctoral Fellow, School of Aerospace Engineering; currently Assistant Professor, Department of Mechanical Engineering, Widener University, Chester, PA. Member AIAA.
‡Graduate Research Assistant, School of Aerospace Engineering. Student Member AIAA.

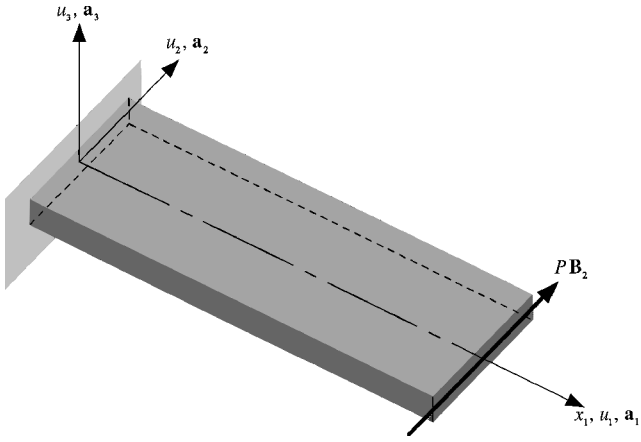

Fig. 1 Schematic of wing showing coordinate systems and follower force.

A load P is applied at the tip of the beam and is directed along unit vector $\boldsymbol{B}_2(\ell, t)$ where $\boldsymbol{B}_2(\ell, t) = -u_2'(\ell, t)\boldsymbol{a}_1 + \boldsymbol{a}_2 + \theta_1(\ell, t)\boldsymbol{a}_3$ and where the prime is the partial derivative with respect to x_1. Thus, the virtual work done by this force through a virtual displacement is

$$\overline{\delta W} = P\boldsymbol{B}_2(\ell, t) \cdot [\delta u_1(\ell, t)\boldsymbol{a}_1 + \delta u_2(\ell, t)\boldsymbol{a}_2 + \delta u_3(\ell, t)\boldsymbol{a}_3]$$
$$= P(-u_2'\delta u_1 + \delta u_2 + \theta_1 \delta u_3)|_0^\ell \tag{1}$$

In keeping with the nonconservative nature of the follower force, there is no potential energy expression, the variation of which will yield this expression for the virtual work. We will subsequently ignore the longitudinal displacement u_1.

For a beam subject to a bending moment $\bar{M}_3$ that is constant in time but varying in x_1, and in which deflections due to that moment are ignored (since $EI_3 \gg EI_2$), the strain energy can be written as

$$U = \int_0^\ell \left[\frac{GJ}{2}\theta_1'^2 + \frac{EI_2}{2}u_3''^2 + \bar{M}_3(u_2'' + \theta_1 u_3'') \right] \mathrm{d}x_1 \tag{2}$$

For static deformation of the beam, one may consider only the first-order terms in $\delta U - \overline{\delta W}$, such that

$$\int_0^\ell (\bar{M}_3 \delta u_2'' - P\delta u_2')\, \mathrm{d}x_1 = 0 \tag{3}$$

Thus,

$$\bar{M}_3 = P(\ell - x_1) \tag{4}$$

as expected. To obtain a weak form that governs static behavior, one may set the second-order terms in $\delta U - \overline{\delta W}$ equal to zero, so that

$$\delta U - \overline{\delta W} = \int_0^\ell [EI_2 u_3'' \delta u_3'' + GJ\theta_1' \delta\theta_1'$$
$$+ P(\ell - x_1)(\theta_1 \delta u_3'' + u_3'' \delta\theta_1)]\, \mathrm{d}x_1 - P\theta_1 \delta u_3|_0^\ell = 0 \tag{5}$$

Integrating by parts, one can eliminate the trailing term so that

$$\delta U - \overline{\delta W} = \int_0^\ell \{EI_2 u_3'' \delta u_3'' + GJ\theta_1' \delta\theta_1' + P[(\ell - x_1)\theta_1]'' \delta u_3$$
$$+ P(\ell - x_1) u_3'' \delta\theta_1\}\, \mathrm{d}x_1 = 0 \tag{6}$$

It can be shown that there is no value of P that will result in buckling. Thus, one must add the kinetic energy and consider the stability of small vibrations about the static equilibrium state.

The kinetic energy of the vibrating beam with mass per unit length of m, radius of gyration of $\bar{\sigma}$, and mass offset $\bar{e}$ is simply

$$K = \frac{1}{2}\int_0^\ell \left(m\dot{u}_2^2 + m\dot{u}_3^2 + m\bar{\sigma}^2\dot{\theta}_1^2 + 2m\bar{e}\dot{\theta}_1\dot{u}_3 \right) \mathrm{d}x_1 \tag{7}$$

where the overdot is the partial derivative with respect to time.

We now undertake a straightforward application of Hamilton's principle,

$$\int_{t_1}^{t_2} (\delta U - \overline{\delta W} - \delta K)\, \mathrm{d}t = 0 \tag{8}$$

where t_1 and t_2 are fixed times. Integrating by parts in time, setting δu_3 and $\delta\theta_1$ equal to zero at the ends of the time interval, removing the time integration, introducing a set of nondimensional variables, and assuming that the motion variables are proportional to $e^{\bar{s}t}$, one obtains a weak form that governs the flutter of a beam subjected to a transverse follower force given by

$$\int_0^1 \left\{ \sqrt{\lambda} w'' \delta w'' + \sqrt{\frac{1}{\lambda}} \theta' \delta\theta' + s^2[w\delta w + e(w\delta\theta + \theta\delta w) \right.$$
$$\left. + \sigma^2 \theta\delta\theta] + p(1-x)w''\delta\theta + p[(1-x)\theta]''\delta w \right\} \mathrm{d}x = 0 \tag{9}$$

where

$$(\,)' = \frac{\mathrm{d}(\,)}{\mathrm{d}x} \qquad x_1 = x\ell \qquad u_3 = \ell w e^{s\psi} \qquad \theta_1 = \theta e^{s\psi}$$
$$\psi = \sqrt{\frac{\sqrt{GJEI_2}}{m\ell^4}}\, t \qquad \lambda = \frac{EI_2}{GJ} \qquad p = \frac{P\ell^2}{\sqrt{GJEI_2}}$$
$$s^2 = \frac{m\ell^4 \bar{s}^2}{\sqrt{GJEI_2}} \qquad \sigma = \frac{\bar{\sigma}}{\ell} \qquad e = \frac{\bar{e}}{\ell} \tag{10}$$

This weak form can be solved approximately by assuming a set of cantilever beam free-vibration modes for bending and torsion. Specifying values for λ, e, and σ, one can solve for the real and imaginary parts of s as functions of p. Given the values chosen for λ, e, and σ, flutter will occur either along with the coalescence of two bending modes or with the coalescence of a bending mode and a torsional mode.

Incorporation of Aeroelastic Effects

The analysis methodology explained in the earlier section solves the problem of instabilities induced by a follower force. One of the goals of the present work is to investigate the instabilities due to the action of both the thrust and the unsteady aerodynamic forces. Such an analysis is quite complex and needs to be done using a numerical solution methodology. The present work uses mixed finite element modeling for the structure and finite state aerodynamic modeling for the unsteady aerodynamics, the details of which are given in Ref. 14 and are not repeated here. The structural model is based on the mixed variational formulation for the dynamics of beams developed by Hodges.[15] When the problem is discretized and simple shape functions are used, the mixed variational formulation leads to an efficient finite element based solution procedure. Various kinds of forces can be applied to the structure, including follower forces and unsteady aerodynamic forces. The follower force is included in a manner similar to the preceding section. The aerodynamic forces are derived from the finite state aerodynamic model of Peters et al.,[16] which gives the unsteady aerodynamic forces on an oscillating airfoil. A two-dimensional aerodynamic model is used because the focus here is on wings with high aspect ratio. A three-dimensional theory may provide higher flutter speeds, making the present results conservative. However, because all of the results obtained in the paper use the same two-dimensional aerodynamic model, the model should be provide adequate predictions of incremental changes of the stability boundary with respect to changes in system parameters. To obtain accurate flutter predictions for wings with low aspect ratio, it would of course be necessary to use a three-dimensional theory. By coupling the structural and aerodynamic models, one obtains a complete aeroelastic analysis methodology. The full finite element equations are linearized about the static equilibrium solution, and an eigenvalue analysis is used to determine the stability of the small motions about static equilibrium.

Results

Results are presented that give insight into the effect of thrust on the flutter characteristics of high-aspect-ratio wings used in high-altitude, long-endurance (HALE) aircraft. The test case is a flexible high-aspect-ratio wing, and Table 1 gives the properties used in the present work. The engine is located near the tip of the wing. Thus, the test case represents an extreme case in which the effects of thrust are maximized. First, the accuracy of the finite element analysis is checked against the analytical solution for the thrust-only case. The results are then presented that include both the aerodynamic effects and the thrust follower force. Next, a parametric study investigating the effect of λ on the flutter boundary is presented. Finally, to put the results in perspective, the thrust required at various trim speeds has been calculated assuming a NACA 0009 airfoil. The thrust required for trim helps in identifying realistic values of the thrust on the wing and thus approximating the percentage change in flutter speed.

Comparison of Analytical and Finite Element Solutions

Before presenting any finite element results that contain aeroelastic effects, the accuracy of the methodology is first validated against the approximate analytical solution for flutter due to thrust only and against the work of Ref. 12. For comparison, the follower force is applied at the tip of the wing for $\lambda = 2$. The approximate analytical solution converges with only a few modes. The converged analytical solution, based on five bending modes and three torsional modes, shows that the critical thrust is 337.2 N. The finite element result using eight elements is 335.1 N, a relative error of 0.6%. This shows that the finite element solution is sufficiently accurate with only eight elements. Moreover, both values agree very well with the analytical solution of Ref. 12.

Next, results from the present analysis are compared with those presented in Ref. 13 for a low-aspect-ratio wing. The data for this test case are given in Table 2. For all cases examined in the absence of aerodynamics, whereas the present analytical solution, the present finite element solution, and the solution of Ref. 12 all agree quite well, Ref. 13 results do not show any flutter instabilities due to thrust only.

The aeroelasticity part of the present finite element methodology was validated in an earlier paper.[14] Unfortunately, as shown in Fig. 2, the results from Ref. 13 do not agree with the present predictions. As discussed earlier, Feldt and Herrmann do not predict a pure thrust-induced instability, whereas the present analysis does, in agreement with that of Ref. 12. Even the pure aeroelastic flutter results do not match. Note that the ordinate and abscissa are the same as the nondimensional parameters used in Ref. 13, which are expressed in terms of those defined in Eq. (10) and, in addition,

$$\mu = m/\rho_\infty \pi b^2, \qquad v = V/b\omega_{\theta_1} \tag{11}$$

where ρ_∞ is the air density, b is the semichord, V is the airspeed, and ω_{θ_1} is the first uncoupled torsional frequency.

The symbols in Fig. 2, and its more detailed blowup in Fig. 3, represent the finite element solution, the analytical solution, and the solution of Ref. 12. It is seen that the thrust required for flutter at negligibly small airspeed (crossing of the flutter boundary curve with the thrust axis) is quite different from that at zero airspeed. The discrepancy is due to two effects. First, the unsteady aerodynamic model predicts forces even at zero airspeed. The forces known as "apparent mass" effects lead to change in the effective mass of the structure and, thus, change in the dynamics and stability characteristics. The symbol denoting the finite element solution does not include the aerodynamic model (air density in the aerodynamic model is set to zero), so that there are no apparent mass terms. That makes this model distinct from one that includes the aerodynamic effects evaluated at a negligibly small airspeed. Second, note that the effect of external damping on the instability of nonconservative systems is quite complex. Even a negligibly small amount of damping has been shown to change the critical force required for instability.[17] In the present case, the small airspeed can provide a small damping to change the critical thrust level.

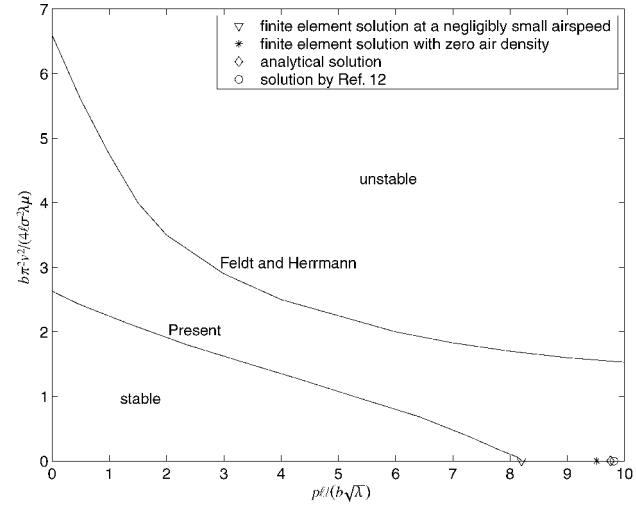

Fig. 2 Comparison with Ref. 13.

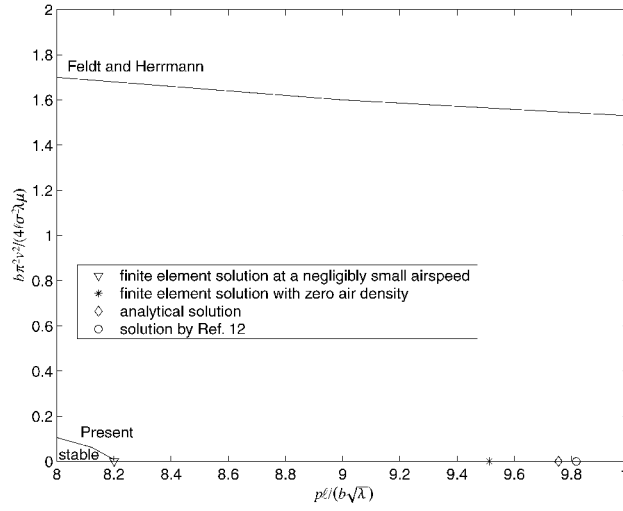

Fig. 3 Comparison with Ref. 13 at very low speed.

Table 1 HALE wing data

Parameter	Value
Half span	16 m
Chord	1 m
Mass per unit length	0.75 kg/m
Moment of inertia (50% chord)	0.1 kg-m
Spanwise elastic axis	50% chord
Center of gravity of wing	50% chord
Bending rigidity (spanwise)	2×10^4 N · m^2
Bending rigidity (edgewise)	4×10^6 N · m^2
Torsional rigidity	Varies with λ
Air density	0.0889 kg/m^3

Table 2 Data from Ref. 13

Parameter	Value
Half span	4 ft (1.219 m)
Chord	1 ft (0.3048 m)
Mass per unit length	0.0132 slug/ft (0.632 Kg/m)
Moment of inertia (elastic axis)	0.0005346 slug-ft (0.002378 Kg-m)
Spanwise elastic axis	39% chord
Center of gravity of wing	42% chord
Bending rigidity	1638.88 lb · ft^2 (677.27 N · m^2)
Torsional rigidity	154.17 lb · ft^2 (63.71 N · m^2)
Air density	0.0011205 slugs/ft^3 (0.57748 Kg/m^3)

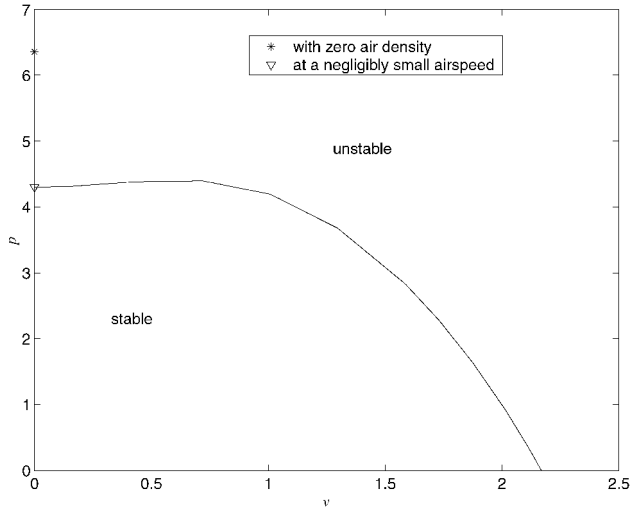

Fig. 4 Flutter boundary for $\lambda = 10$.

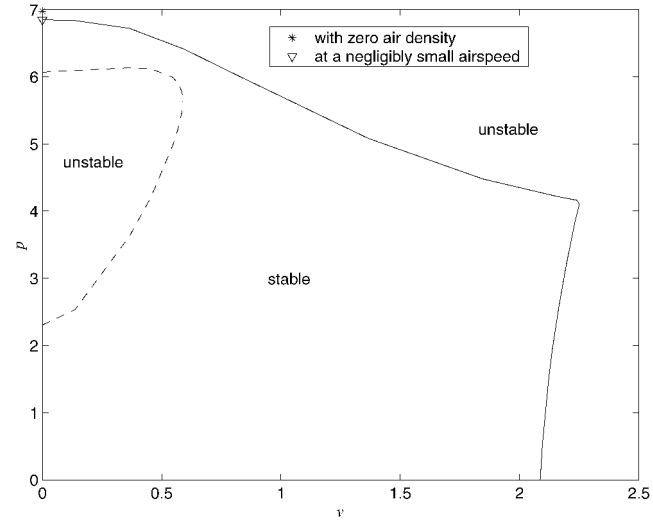

Fig. 5 Flutter boundary for $\lambda = 1$.

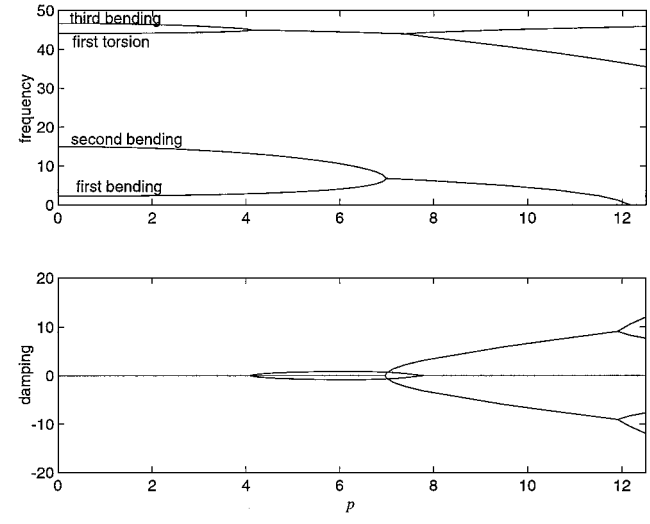

Fig. 6 Frequency and damping at $\lambda = 1$.

Change in Flutter Speed with Thrust

The finite element methodology is now used to investigate the effect of thrust on the flutter speed of a cantilevered wing. The thrust is applied at 15 m from the root, that is, 1 m from the tip of the wing. The flutter boundary is plotted by first selecting a level of thrust, followed by solving the nonlinear steady state. Once the steady-state solution is obtained, the problem is dynamically linearized about the steady state to get a set of linear equations of motion in terms of the perturbation quantities. The flutter analysis is then conducted to obtain the flutter speed. This presupposes that the airspeed has a weak effect on the steady-state solution, which is correct in all cases we examined.

Figure 4 shows the flutter boundary for $\lambda = 10$. All results of the flutter boundary presented from here on are plotted in terms of the nondimensional force p [as defined in Eq. 10)] and the standard reduced airspeed v [as defined in Eq. (11)]. It is seen that there is a continuous decrease in the flutter speed with increase in thrust. From another perspective, one can say that there is a continuous decrease in the magnitude of thrust required for instability with increase in airspeed. This can be qualitatively explained as the addition of the destabilizing effects of the two forces (aerodynamic and follower force) leading to instability at lower levels of the forces. The symbol denoting the finite element solution points out the critical thrust without aerodynamic effects. Again, at zero airspeed, there is a jump in flutter force, that is a small offset from zero airspeed leads to a sudden decrease of the flutter force. As explained earlier, this is because when aerodynamic forces are included, even at zero airspeed, there is a slight shift in the dynamic properties due to the apparent mass of the air and the effect of negligibly small aerodynamic damping.

Excellent agreement was obtained between the finite element and approximate analytical solutions for a wide range of parametric values. The one exception to this is indicated in Fig. 5, which shows the flutter boundary for $\lambda = 1$. The dashed line is a small unstable regime predicted by the finite element method that, for reasons unknown, is not predicted by the approximate analytical solution. Figure 6 shows the frequency and damping (imaginary and real part of the eigenvalues) of the system without aerodynamics. It is clear that the unstable region is due to the coalescence of the first torsion mode with the third bending mode. The frequency of this mode is much higher than the few modes retained in the approximate analytical solution. However, even when a larger number of modes is retained, the approximate analytical solution is unable to capture it. Moreover, attempts to link this regime with edgewise flexibility effects also failed. It is clear, however, that a very small amount of structural damping will eliminate this instability, and so it is not of practical importance. Thus, only the low-frequency flutter modes will be considered henceforth.

An important observation can be made from Figs. 4 and 5. Unlike the $\lambda = 10$ case, the critical airspeed for $\lambda = 1$ does not monotonically decrease with an increase in thrust. Rather, there is a reversal. For low levels of thrust, the flutter speed increases, but, as the thrust level is increased further, one sees a change in mode of instability from a dominant aeroelastic mode to a dominant follower force instability. Afterward there is a decrease in the flutter speed with thrust, culminating in the zero speed flutter at the pure follower force instability. To ascertain what is going on here, one needs to vary λ more systematically. The effect of several values of λ on the flutter boundary is shown in Fig. 7. It is seen that the interactions between the thrust and aeroelastic destabilization mechanisms are quite different for lower values of λ, for example, 1, 1.5, and 2, as compared to the higher values, for example, 10 and 15. Figure 7 shows these trends changing from one type to the other around $\lambda = 5$. With a careful look at the flutter boundary for $\lambda = 5$, one can see that there is still a range where thrust level increases with airspeed, but it does not show a sudden transition of the flutter frequency as in the cases where $\lambda < 5$.

Change in Flutter Speed with λ

To understand the difference in the behavior of the wing at the different λ, one needs to look at the modes involved in the instability mechanisms. Figure 8 shows the evolution of the pure follower force instability for $\lambda = 2$. For lower λ, the lowest follower-force instability exhibits a bending–bending frequency coalescence. Figure 9 shows a similar plot for $\lambda = 10$, which on the other hand, exhibits an instability due to a torsion–bending frequency coalescence. Modal

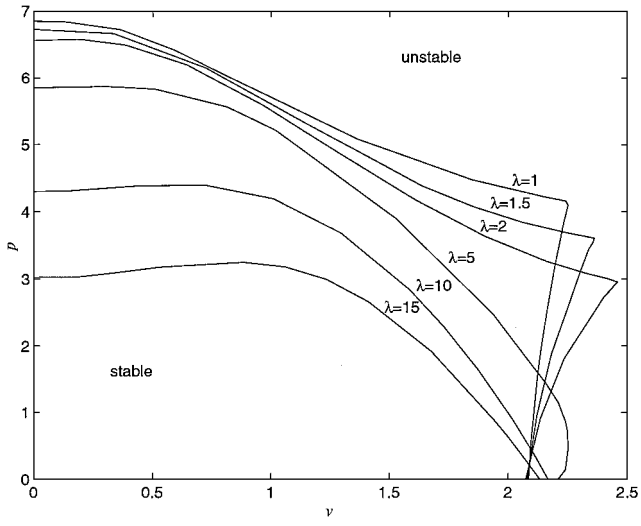

Fig. 7 Effects of λ variation on flutter.

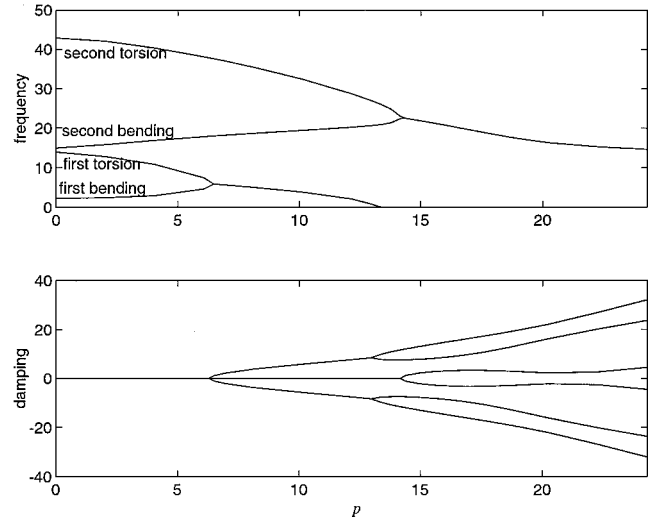

Fig. 9 Eigenanalysis of follower force at $\lambda = 10$.

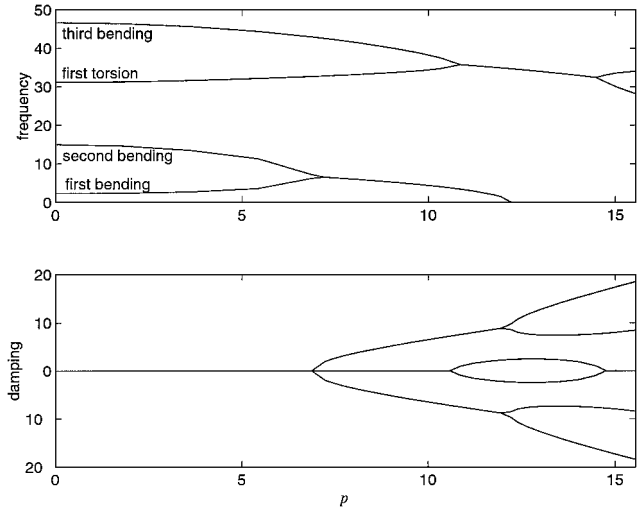

Fig. 8 Eigenanalysis of follower force at $\lambda = 2$.

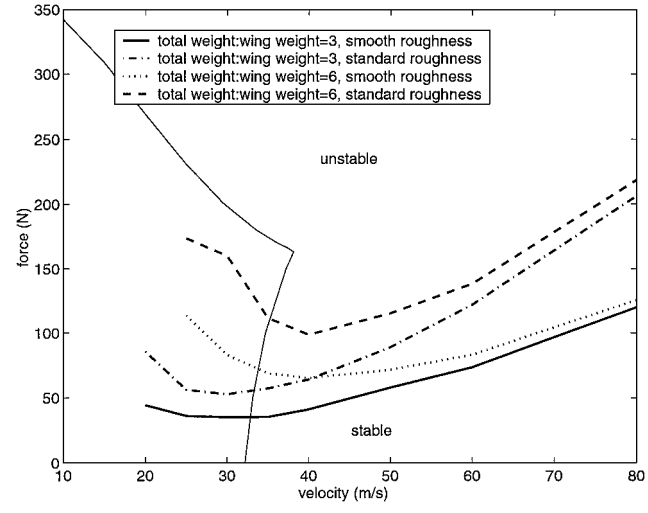

Fig. 10 Flutter range for HALE wing at $\gamma = 0.8$ and $\lambda = 2$.

analysis of pure aeroelastic instabilities show that, in both cases, the pure aeroelastic instabilities come from first torsional modes. The results can be explained qualitatively as follows: Near the aeroelastic flutter speed, the instability for $\lambda = 2$ is less affected by the thrust (than the one for $\lambda = 10$) because different modes are involved in the aeroelastic instability and the follower force instability. For $\lambda = 10$, the torsion–bending instability from pure follower force interacts with the pure aeroelastic torsion instability involving the same modes, thereby decreasing the flutter speed as thrust level increases.

Trim Solution and Actual Flutter Range

Finally, some points need to be made regarding the levels of thrust on an actual aircraft to put the results presented in the earlier sections in the correct perspective. Required thrust to maintain trimmed flight is calculated by assuming a NACA 0009 as the wing airfoil and considering both smooth and standard roughness values at the same Reynolds number. The value of roughness affects the drag coefficient significantly.[18] The ratio of total airplane weight to twice the wing weight is taken to be either 3 or 6. This is useful in calculating the weight of the aircraft and, thus, in estimating the lift and then the drag using the roughness. Here γ is defined as the ratio of fuselage drag over total drag. Note that the flutter calculation does not make use of γ, that is, the nonlinear drag effects were neglected. Here, γ is used to calculate the total drag (and thus the thrust required) using the wing drag. The wing drag is calculated using the lift-to-drag ratio for the given smoothness. The lift equal to the total weight is in turn calculated using the airplane-to-wing weight ratio. The flutter boundary is shown in Fig. 10 for $\gamma = 0.8$. Also plotted are the velocity–thrust curves for various smoothness and airplane weight factors. The aeroelastic flutter speed without thrust is 32.21 m/s. The flutter speed including the thrust effects for standard roughness and high fuselage mass is 35.8 m/s. Thus, incorporation of thrust can change the predicted flutter speed by 11%. Figure 10 shows practical levels of thrust and the corresponding flutter speed for various conditions. In an actual aircraft, one would use the thrust levels known for trim flight to estimate the changes in flutter speed.

Conclusion

There has been a large amount of published work dealing with the stability analysis of a tangential follower force, but there has been very little study on the influence of a lateral follower force on aeroelastic flutter. An analytical solution for the in vacuo case was developed and shown to match closely results from the numerical method. A parametric study of thrust effects on aeroelastic flutter was performed. Whether or not thrust is stabilizing depends strongly on λ, the ratio of bending stiffness to torsional stiffness. For $\lambda \leq 5$, it was shown that thrust up to a certain value can increase flutter speed. However, for $\lambda \geq 10$, thrust always decreases flutter speed. Moreover, the shape of flutter curve is greatly affected by λ.

The present work does not consider several aspects of the system that may be important to obtain accurate results for realistic cases.

These may include, but are not limited to, engine mass and inertia, engine gyroscopic effects, and location of the engine at different points along the wing. However, based on the present work, which is indeed preliminary, the flutter speed was shown to vary as much as 11% for the case of a high-aspect-ratio wing. Therefore, in general, it would appear prudent to include this effect in general-purpose flutter analyses.

References

[1]Goland, M., "The Flutter of a Uniform Cantilever Wing," *Journal of Applied Mechanics*, Vol. 12, No. 4, 1945, pp. A197–A208.

[2]Fung, Y. C., *An Introduction to the Theory of Aeroelasticity*, Wiley, New York, 1955, Chap. 5.

[3]Bisplinghoff, R. L., Ashley, H., and Halfman, R. L., *Aeroelasticity*, Addison Wesley Longman, Reading, MA, 1955, Chap. 9.

[4]Beck, M., "Die Knicklast des einseitig eingespannten, tangential gedrückten Stabes," *ZAMP*, Vol. 3, No. 3, 1952, pp. 225–288.

[5]Bolotin, V. V., *Nonconservative Problems of the Theory of Elastic Stability*, Pergamon, New York, 1963, Chap. 2.

[6]Leipholz, H. H. E., *Stability of Elastic Systems*, Sijthoff and Noordhoff, Alphen aan den Rijn, The Netherlands, 1980, Chap. 4.

[7]Chen, L.-W., and Ku, D.-M., "Eigenvalue Sensitivity in the Stability Analysis of Beck's Column with a Concentrated Mass at the Free End," *Journal of Sound and Vibration*, Vol. 153, No. 3, 1992, pp. 403–411.

[8]Park, Y. P., "Dynamic Stability of a Free Timoshenko Beam Under a Controlled Follower Force," *Journal of Sound and Vibration*, Vol. 113, No. 3, 1987, pp. 407–415.

[9]Higuchi, K., "An Experimental Model of a Flexible Free–Free Column in Dynamic Instability Due to an End Thrust," *Proceedings of the 35th AIAA/ASME/ASCE/AHS/ASC Structures, Structural Dynamics, and Materials Conference*, AIAA, Washington, DC, 1994, pp. 2402–2408.

[10]Kim, J.-H., and Choo, Y.-S., "Dynamic Stability of a Free–Free Timoshenko Beam Subjected to a Pulsating Follower Force," *Journal of Sound and Vibration*, Vol. 216, No. 4, 1998, pp. 623–636.

[11]Como, M., "Lateral Buckling of a Cantilever Subjected to a Transverse Force," *International Journal of Solids and Structures*, Vol. 2, 1966, pp. 515–523.

[12]Wohlhart, K., "Dynamische Kippstabilität eines Plattenstreifens unter Folgelast," *Zeitschrift für Flugwissenschaften*, Vol. 19, No. 7, 1971, pp. 291–298.

[13]Feldt, W. T., and Herrmann, G., "Bending–Torsional Flutter of a Cantilevered Wing Containing a Tip Mass and Subjected to a Transverse Follower Force," *Journal of the Franklin Institute*, Vol. 297, No. 6, 1974, pp. 467–478.

[14]Patil, M. J., Hodges, D. H., and Cesnik, C. E. S., "Nonlinear Aeroelastic Analysis of Complete Aircraft in Subsonic Flow," *Journal of Aircraft*, Vol. 37, No. 5, 2000, pp. 753–760.

[15]Hodges, D. H., "A Mixed Variational Formulation Based on Exact Intrinsic Equations for Dynamics of Moving Beams," *International Journal of Solids and Structures*, Vol. 26, No. 11, 1990, pp. 1253–1273.

[16]Peters, D. A., Karunamoorthy, S., and Cao, W.-M., "Finite State Induced Flow Models; Part 1: Two-Dimensional Thin Airfoil," *Journal of Aircraft*, Vol. 32, No. 2, 1995, pp. 313–322.

[17]Herrmann, G., and Jong, I.-C., "On the Destabilizing Effect of Damping in Nonconservative Elastic Systems," *Journal of Applied Mechanics*, Vol. 32, No. 3, 1965, pp. 592–597.

[18]Anderson, J. D., *Introduction to Flight*, 2nd ed., McGraw–Hill, New York, 1985, p. 549.